Molecular Bases of Disease:

# Mitochondrial dysfunction and decrease in body weight of a transgenic knock-in mouse model for TDP-43


Carola Stribl, Aladin Samara, Dietrich Truembach, Reginas Augustin, Manuela Neumann, Helmut Fuchs, Valerie Gailus-Durner, Martin Hrabe de Angelis, Birgit Rathkolb, Eckhard Wolf, Johannes Beckers, Marion Horsch, Frauke Neff, Elisabeth Kremmer, Sebastian Koob, Andreas S. Reichert, Wolfgang Hans, Jan Rozman, Martin Klingenspor, Michaela Aichler, Axel Karl Walch, Lore Becker, Thomas Klopstock, Lisa Glasl, Sabine M. Holter, Wolfgang Wurst and Thomas Floss

*J. Biol. Chem.* published online February 10, 2014

---

Access the most updated version of this article at doi: 10.1074/jbc.M113.515940

JBC Papers in Press. Published on February 10, 2014 as Manuscript M113.515940
The latest version is at http://www.jbc.org/cgi/doi/10.1074/jbc.M113.515940

# Mitochondrial dysfunction and decrease in body weight of a transgenic knock-in mouse model for TDP-43

**Carola Stribl (1), Aladin Samara (1), Dietrich Trümbach (1), Regina Augustin (1), Manuela Neumann (2); Helmut Fuchs (3), Valerie Gailus-Durner (3), Martin Hrabě de Angelis (3,7,14), Birgit Rathkolb (3,4), Eckhard Wolf (4), Johannes Beckers (3,7), Marion Horsch (3), Frauke Neff (5), Elisabeth Kremmer (6), Sebastian Koob (8), Andreas S. Reichert (8,15), Wolfgang Hans (3,11), Jan Rozman (3,11), Martin Klingenspor (11), Michaela Aichler (12), Axel Karl Walch (12), Lore Becker (3, 13), Thomas Klopstock (9,13,14), Lisa Glasl (1), Sabine M. Hölter (1,7), Wolfgang Wurst (1,7,9,10) and Thomas Floss (1,7)**

(1) Helmholtz Zentrum München, Institute of Developmental Genetics, Ingolstädter Landstrasse 1, 85764 Neuherberg, Germany; (2) Institute of Neuropathology, Schmelzbergstr. 12, CH-8091 Zurich, Switzerland; (3) Helmholtz Zentrum München, German Mouse Clinic, Institute of Experimental Genetics, Ingolstaedter Landstrasse 1, 85764 Neuherberg, Germany; (4) Chair for Molecular Animal Breeding and Biotechnology, Gene Center, Ludwig-Maximilians-Universität München, 81377 Munich, Germany (5) Helmholtz Zentrum München, German Mouse Clinic, Institute of Pathology, Ingolstaedter Landstrasse 1, 85764 Neuherberg, Germany; (6) Helmholtz Institut für Molekulare Immunologie (IMI), (7) Technische Universität München; c/o Helmholtz Zentrum München, (8) Buchmann Institute for Molecular Life Sciences, Mitochondrial Biology, Max-von-Laue-Str. 15, 60438 Frankfurt am Main, Germany and Mitochondriale Biologie, Zentrum für Molekulare Medizin, Goethe Universität Frankfurt am Main, Theodor-Stern-Kai 7, 60590 Frankfurt am Main, Germany (9) Deutsches Zentrum für Neurodegenerative Erkrankungen e. V. (DZNE), Site Munich, Schillerstrasse 44, D-80336 Munich, Germany, (10) Max-Planck-Institute of Psychiatry, Kraepelinstr. 2-10, 80804 München, Germany, (11) Molecular Nutritional Medicine, Else Kröner Fresenius Center and ZIEL Research Center for Nutrition and Food Science, Technische Universität München, Gregor-Mendel-Str. 2, 85350 Freising – Weihenstephan, Germany (12) Research Unit Analytical Pathology, Institute of Pathology, Helmholtz Zentrum München, (13) Department of Neurology, Friedrich-Baur-Institute, Ludwig-Maximilians-Universität, Ziemssenstr.1a, 80336 Munich, Germany, (14) German Center for Vertigo and Balance Disorders, Munich, Germany, (15) Mitochondriale Biologie, Zentrum für Molekulare Medizin, Goethe Universität Frankfurt am Main, Max-von-Laue-Str. 15, 60438 Frankfurt am Main, Germany.

Running title: *"Knock-in" mouse of TDP-43 displayed altered fatty acid metabolism.*

To whom correspondence should be adressed: Thomas Floss, Helmholtz Zentrum München, Institute of Developmental Genetics, Ingolstädter Landstrasse 1, 85764 Neuherberg, Germany. Tel. +498931872887; Fax: +498931873099; tfloss@helmholtz-muenchen.de.

**Keywords**: Tardbp/TDP-43, Frontotemporal Dementia (FTD), Amyotrophic Lateral Sclerosis (Lou-Gehrig's disease; ALS), Recombinase-mediated cassette exchange (RMCE).

---

**Background**: Mutations in TDP-43 are frequently found in ALS patients.
**Results**: A315T TDP-43 protein is elevated from this transgenic knock-in allele due to disturbed feedback regulation.
**Conclusion**: Elevation of A315T TDP-43 was insufficient to cause ALS in this mutant.
**Significance**: This TDP-43 allele could be valuable in determining genetic or environmental factors that cause full-blown FTD or ALS.

**Abstract**

**The majority of Amyotrophic Lateral Sklerosis (ALS) cases as well as many patients suffering from Frontotemporal Lobar Dementia (FTLD) with ubiquitinated inclusion bodies show TDP-43 pathology, the protein encoded by the TAR-DNA binding protein (*Tardbp)* gene. We used recombinase-mediated cassette exchange (RMCE) to introduce an ALS patient cDNA into the mouse Tdp-43 locus. Expression levels of human A315T TDP-43 protein were 300% elevated in heterozygotes while the endogenous mouse Tdp-43 was decreased to 20% of wildtype levels as a result of disturbed feedback regulation. Heterozygous TDP-43$^{A315TKi}$ mutants lost 10% of their body weight and developed insoluble TDP-43 protein starting as early as 3 months after birth, a pathology that was exacerbated with age. We analyzed the splicing patterns of known Tdp-43 target genes, as well as genome-wide gene expression levels in different tissues that indicated mitochondrial dysfunction. In heterozygous mutant animals we observed a relative decrease in expression of Parkin (Park2) and the fatty acid transporter CD36 along with an increase in fatty acids, HDL cholesterol and glucose in the blood. As seen in Transmission Electron Microscopy, neuronal cells in motor cortices of TDP-43$^{A315TKi}$ animals had abnormal neuronal mitochondrial cristae formation. Motor neurons were reduced to 90% but only slight motoric impairment was detected. The observed phenotype was interpreted as a predisease model which might be valuable for the identification of further environmental or genetic triggers of neurodegeneration.**

---

**Introduction**

The *Tardbp* gene codes for TDP-43, a RNA-binding protein of 43kDa which has been implicated in a number of neurodegenerative diseases such as Frontotemporal Lobar Dementia (FTLD) and Amyotrophic Lateral Sclerosis (ALS) but also Chorea Huntington (HD), Alzheimer's Disease (AD) and Parkinson's Disease (PD) [1-8]. TDP-43 is a widely expressed hnRNP with two RNA-recognition motifs (RRM) and high affinity to single-stranded nucleic acids [9-14]. Although predominantly located in the nucleus, TDP-43 shuttles between the nucleus and the cytoplasm under normal conditions [15]. In the nucleus, TDP-43 is involved in microRNA biogenesis [16] and splicing regulation where it causes exon inclusion or exclusion, depending on number and localization of its GT-enriched target sequences [17-22]. Upon stress exposure TDP-43 is recruited to stress granules (SG) in cultured cells which serve as cytoplasmic storage of RNAs to become instantly available for translation without further transcription processes [10, 23-25]. Under pathological conditions, TDP-43 is ubiquitinated, phosphorylated and forms neuronal cytoplasmic inclusions (NCI) in upper and lower motor neurons [26-27]. The vast majority of ALS mutations has been observed in the glycine-rich domain of TDP-43, a domain which is thought to function in protein-protein interaction, as TDP-43 interacts with a large number of proteins, including itself under physiological conditions [28-30]. Cellular steady-state levels of TDP-43 are mainly regulated through a TDP-43 auto-feedback [17, 31-32]. High levels of TDP-43 are toxic to cells, yet also low TDP-43 levels are not tolerated [11, 33-34]. Hence, transgenic overexpressors downregulated endogenous TDP-43 levels while heterozygous TDP-43 knockout mice showed an increased expression of the wildtype allele. A number of transgenic mice expressing wildtype or mutant human TDP-43 have been established, showing either early lethality or severe motor dysfunction shortly after birth [35-37]. No mouse model so far has shown all the features of ALS. It is not yet clear, under which conditions TDP-43 pathology develops *in vivo* and what the role of the mutations for the progression of the disease is. In order to investigate the role of a TDP-43 mutation under physiological conditions, we generated a mouse line expressing a human TDP-43

cDNA, carrying an A315T mutation under the control of the endogenous *Tardbp* promoter.

## Experimental Procedures

### Generation of hTDP-43$^{A315T}$ mice

Animals were generated via RMCE as previously described [38]. Briefly, the final exchange vector was established from pENTR-Ex containing full-length cDNA TDP-43(A315T) and pEX-Dest in a Gateway reaction using clonase and following standard protocols (Invitrogen). Transfection was performed using the FlEx conditional GGTC gene trap clone D045A10. Hygro-resistant clones were screened for successful exchange by PCR using internal oligonucleotides in the splice acceptor of pEX-FLP-hTDP-43(A315T) and in the 5'-LTR. *In vivo* excision of hygromycin by Cre was done using Rosa26Cre transgenic mice (Taconic; 006467-T-F Heterozygous C57BL/6NTac-$^{Gt(ROSA)26Sortm16(cre)Arte}$).

### Genotyping

Mice expressing human A315T TDP-43 protein were identified by PCR using following primers: D045for 5'-CTGTTGTCGGATTCCTTCCC-3', D045rev 5'-CTCGTCATTTCTTACCTGGAG-3' and LTR for 5'-CAACTGCAAGAGGGTTTATTGG-3'

### Quantitative real-time PCR

Levels of mouse and human TDP-43 transcripts were determined using commercial TaqMan® Gene Expression Assays (Applied Biosystems). Total RNA was extracted from frozen brain tissue using TRIzol® (Invitrogen) and RNeasy Mini Kit (Qiagen). Total RNA was treated with DNase (Qiagen) to eliminate genomic DNA. 1 µg of RNA was used to synthesize cDNA using the High Capacity cDNA Reverse Transcription Kit (Applied Biosystems). Following gene expression assays were used: hTDP-43 Hs0606522_m1, mTDP-43 Mm00523866_m1 and mouse ACTB (endogenous control, 4352933E) (Applied Biosystems).

### Western Blotting

For soluble fractions tissues were homogenized in RIPA buffer (50mM Tris-HCl, pH 7.4, 150mM NaCl, 1% Triton X-100, 0.5% Sodium Deoxycholat, 1% SDS, 3mM EDTA and protease and phosphatase inhibitor cocktail) and sonicated. Following centrifugation supernatant was assessed by BCA protein assay kit (Thermo Scientific). The pellet was twice redissolved in RIPA buffer, sonicated and centrifuged at 100,000xg at 4°C for 30 min. Finally the pellet was resuspended in urea buffer (7M urea, 2M thiourea, 4% CHAPS, 30mM Tris-HCl, pH 8.5), sonicated and centrifuged at 20,000xg at RT for 30 min. The supernatant was used for the insoluble fraction. Equal amounts of protein were loaded on a Nu-PAGE 4-12% Bis-Tris gel (Invitrogen) and transferred on a nitrocellulose membrane. Following antibodies were used: rabbit anti-TDP-43 antibody (ProteinTech, 10782-2-AP; 1:1000), human specific mouse anti-TDP-43 antibody (Abcam, ab57105; 1:1000), mouse anti-parkin antibody (Santa Cruz Biotechnology,Inc. 1:1000), rat anti-TDP43 phosphorylated (1D3; E. Kremmer, 1:100) [39], mouse anti-FUS (Santa Cruz Biotechnology Inc., 1:1000), mouse anti-Ubiquitin (Millipore, 1:500), rabbit anti-p62 (Santa Cruz, sc-25575), anti-Opa1 (BD Biosciences), anti-CD36 (R&D Systems, 1:500). Detection was performed using HRP-conjugated secondary antibodies and ECL Plus Chemiluminescent Detection System (Amersham Biosciences). Data were normalized to mouse anti-β-actin (GeneTex, 1:10000).

### Immunohistochemistry/Immunofluorescence

Mice were perfused transcardially using 4% paraformaldehyde in 0.1M phosphate buffer and paraffin-embedded. Eight-micrometer sections of brain and spinal cord were cut. For immunohistochemistry, the tissue was quenched in 0.2% $H_2O_2$ in PBS and antigen-retrieval was done with citrate buffer for 1h.

After blocking in 10% normal goat serum for 1h at room temperature, primary antibodies were incubated overnight at 4°C. The tissue was treated with biotinylated secondary antibodies (1:300) for 1h at room temperature, incubated in avidin-biotin complex (Vector Laboratories) and developed using DAB (Sigma). Nissl- and hematoxylin/eosin staining were performed using standard methods.
Double immunofluorescence was performed on fixed paraffin-embedded sections of the brain and spinal cord using the described primary antibodies and Alexa Fluor 594 or 488-conjugated secondary antibodies.

**Transmission Electron microscopy**.

Animals were perfused as described in the immunhistochemistry section. Tissue samples were fixed in 2.5% electron microscopy grade glutaraldehyde in 0.1 M sodium cacodylate buffer pH 7.4 (Science Services, Munich, Germany), postfixed in 2% aqueous osmium tetraoxide, dehydrated in gradual ethanol (30–100%) steps and propylene oxide, embedded in Epon (Merck, Darmstadt, Germany) and cured for 24 hours at 60°C. Semithin sections were cut and stained using toluidine blue. Ultrathin sections of 50 nm were collected onto 200 mesh copper grids, stained using uranyl acetate and lead citrate prior to transmission electron microscopy examination (Zeiss Libra 120 Plus, Carl Zeiss NTS GmbH, Oberkochen, Germany). Pictures were acquired using a Slow Scan CCD-camera and iTEM software (Olympus Soft Imaging Solutions, Münster, Germany).

**ES cell culture**
All clones were derived from feeder independent E14 Tg2A.4 cells [40] gene trap lines, with the exception of D045A10 which was derived from a TBV2 cell line [41] and was cultured on a mouse embryonic fibroblast feeder layer. ES cells lines were grown under standard culture conditions (http://www.genetrap.de). For Cre transfection the exchange clones were transfected with 50µg of supercoiled Caggs-CRE-IRES-Puro plasmid. After electroporation, ES cells were plated on gelatine-coated culture dishes ($1x10^3$, 100mm) for 3 to 4 days. Selected colonies were transferred to 96-well plates and expanded in three replicates to 96-wells. One plate was used for the isolation of genomic DNA and genotyping. Positive clones were expanded on gelatine-coated 100mm dishes and used for protein analysis.

**Behavioural tests**
All behavioural tests were carried out as described previously [42-43].
*Beam Walk.* Mice were trained to traverse a 1-m wooden round beam. After the training period animals were placed on the beam for five testing trials. Time needed to traverse the beam, number of foot slips and number of falls off the beam were measured.
*Vertical Pole Test.* The animals were placed head upwards on a 50-cm high, taped pole. The time needed to turn downwards and to descend were measured.
*Accelerating Rotarod.* Mice were placed on a rod rotating at 4 rpm constant speed. Rotation speed was accelerated from 4 to 40 rpm in 300 s. Latency and rpm at which each mouse fell off were recorded. The test phase consisted of three trials separated by 15 min inter-trial intervals.
*Ladder.* Animals were placed on a horizontal ladder on which spacing of the rungs is variable. After a short training period, mice needed to traverse the ladder. The number of front and hind paws slips and time to cross the ladder were recorded.
*Gait analysis.* Mice performed three uninterrupted runs in a dark room over an elevated glass walkway. The footprint pattern was tracked by a camera (Pulnix Camera RM-765) and analysed using the "Cat Walk" software Version 7.1.
*Y-maze.* The Y-maze is an apparatus by the shape of a Y, encompassing three identical arms connected with a triangular platform. The mice were placed at the end of one arm and allowed to explore the Y-maze for a five minute interval. Latency to leave the first arm, total number and sequence of entries into each arm were counted.

*Object recognition.* Two identical objects were placed in an empty arena and the mice were allowed to explore them for 5 min. Each mouse had three sampling trials with inter-trial intervals of 15 min. At 3 and 24 hours after the third sampling trial, one object was replaced by a new, unfamiliar one. The exploration times were scored for each trial and analysed.

**MN counting**

For spinal motor neuron quantification mice were perfused with 4% paraformaldehyde and the spinal cord was removed and embedded in paraffin. Serial 8µm sections from the L3-L5 region were cut. Sections were Nissl stained and every second section was used for counting motor neurons in the sciatic motor pool. Only cells with a clear, definable nucleolus were scored.

**Rapid amplification of cDNA ends (3'RACE)**

Total RNA was isolated from adult brain tissue as described above. Reverse transcription and 3'RACE were performed with the FirstChoice®RLM-RACE Kit (Ambion) using following gene specific primer: 5'-ATATTCTGCCATAGGAATAC -3'

**Clinical Chemistry**

A cohort of 40 mice, 20 mice per sex, and an equal number of wildtype littermates was phenotypically analyzed within the German Mouse Clinic (GMC) in a two-pipeline systematic primary phenotyping screen using ten mice per group being utilized for each test. In the following, only tests resulting in the detection of significant genotype-related differences are described in detail: Blood samples were collected by retrobulbar puncture from isoflurane anesthetized mice into heparinized tubes in both pipelines. Mice analyzed in pipeline 1 were fasted overnight for 16 to 18 hours prior to blood collection. Blood samples collected from fasted mice were stored after collection in a rack on wet ice for not longer than one hour until being separated by centrifugation and plasma was immediately frozen at -80°C until analysis. Samples collected from ad libitum fed mice in pipeline 2 were stored one to two hours at room temperature before centrifugation (10 minutes at 8°C, 5000 x g, Biofuge fresco, Hereaus) and plasma was distributed for the different blood-based screens. Clinical chemistry analysis of these samples was performed on the day of collection using 1:2 diluted samples. Clinical chemical parameters were determined using an AU400 autoanalyzer (Olympus, Germany, distributed by Beckman-Coulter in the meantime) and adapted reagents from Beckman-Coulter, Wako and Randox. Plasma samples collected from overnight fasted mice were analyzed for concentrations of total cholesterol, HDL-cholesterol, triglyceride, glucose, non-esterified fatty acids (NEFA) and glycerol, while a set of 18 parameters (concentrations of sodium, chloride, potassium, calcium, inorg. phosphorus, iron, total protein, albumin, urea, creatinine, total cholesterol, triglyceride, and glucose, as well as plasma activities of ALAT, ASAT, AP, α-amylase and LDH) was measured in samples collected in pipeline 2.

**Molecular Phenotyping**

Brain and muscle were collected from mice at the age of 17 weeks. Total RNA of the different organs was isolated from eight (testis) and fourteen (brain) mice (four/six mutant and four/eight wild type mice) according to manufacturer's protocol using RNeasy Mini kits (Qiagen). RNA integrity was monitored on a formaldehyde agarose gel and concentration calculated from $OD_{260/280}$ measurement. 500ng of this high quality total RNA were amplified using the Illumina TotalPrep RNA Amplification kit (Ambion). The amplified cRNA was hybridised to MouseRef-8 v2 Expression BeadChips (Illumina, San Diego, CA, USA) and subsequent to 16 hours incubation, staining and scanning were done according to the Illumina expression protocol. Data was normalized using the GenomeStudioV2011.1 software and processed using the quantile normalisation, background subtraction option and introduction of an offset to remove remaining negative expression values. The identification of significant gene regulation was per-

formed using SAM (Significant Analysis of Microarrays) included in the TM4 software package. Genes were ranked according to their relative difference value d(i), a score assigned to each gene on basis of changes in gene expression levels in relation to the standard deviation. Genes with d(i) values greater than a threshold were selected as significantly differentially expressed in an one class analysis. The percentage of such genes identified by chance is the false discovery rate (FDR). To estimate the FDR, nonsense genes were identified by calculation of 1000 permutations of the measurements. The selection of the top differentially expressed genes with reproducible up- or down-regulation includes about 5% false positives (FDR) in combination with fold change > 1.4. Array data are available in the GEO database (http://www.ncbi.nlm.nih.gov/geo/?roo=md) under GSE39585.

**Bioinformatics Analysis**

Support Vector Machines with Recursive Feature Elimination (SVM-RFE) according to Zhou et al. (2007) [44] was performed on normalized microarray data of TDP-43 mutant and wildtype mice. For SVM prediction the function svm from the e1071 package in R (http://www.r-project.org/) was used with default settings except the parameters type = 'C-classification', kernel = 'linear' and cost = 0.1. SVM-RFE algorithm grouped the samples of the microarray dataset (six wildtype and six mutant animals) into stratified five folds and all combinations of four folds were used for mSVM-RFE. The grouping into folds was done ten times and the SVM-RFE algorithm was applied 50 times on different subsets of the original dataset. Finally, 50 different probeset selections, each consisting of the best 500 probesets for classification according to the cost function of the SVM classifier were obtained. The frequency of each occurring in all the probeset selections was computed to identify the most important (see detailed description of an application of this algorithm in Augustin et al. 2011[45]).

Differentially expressed genes occurring in at least 15 selections were functionally investigated with the Ingenuity Pathway Analysis software (IPA content version: 12710793, Release Date: 2012-05-07) and explored for enrichment in Gene Ontology (GO) categories cellular component and biological process [46] by the program Pathway Studio 9.0 (Ariadne Genomics). For calculation of p-values a Fisher's exact test was performed with both tools.

**Results**

**Increased TDP-43 levels in mice expressing hTDP-43$^{A315T}$**

To study the pathological functions of A315T TDP-43 protein, we generated mice expressing human TDP-43 cDNA with the A315T mutation under control of the endogenous *Tardbp* promoter [38]. The hTDP-43$^{A315T}$ +/- mice were viable and fertile. hTDP-43$^{A315T}$ +/- mice were intercrossed to generate homozygous mutants. However, no homozygous hTDP-43$^{A315T}$ mice were identified among 200 pups genotyped at weaning age. To determine the stage of lethality, 20 embryos were genotyped at embryonic day E7.5 after het x het matings. Again no homozygous mutant embryos were found indicating lethality of homozoygotes before or around gastrulation (E6.5 – E7.5; Fig. 1A). Therefore, this entire study was done using heterozygotes. Expression levels of TDP-43 were found to be elevated in the adult brain and yet in a variety of other tissues of the mutants, too (Fig. 1B,C). We detected two tissue specific TDP-43 isoforms in Western blots. Due to the presence of a smaller TDP-43 isoform in the kidney (35kDa), which was detectable with an antibody recognizing the N-terminus of human TDP-43 protein, and the fact that a human cDNA was expressed, we concluded that the 35kDa form was not a result of alternative splicing but rather represents a C-terminal post-translational truncation. The second tissue-specific isoform was a 60kDa band which was detectable only in the brains of wildtype and heterozygous animals. To date, the nature of this band is still unclear (Fig. 1B). To investigate the onset of TDP-43 overexpres-

sion we analyzed brain lysates from 1, 6 and 12 months old mutants. Elevated TDP-43 protein amounts, which were estimated to 2.5x of wild-type levels from Western blots, were already present in one month old heterozygotes (Fig. 1C). Next, we examined the relative levels of the mouse and the mutant human TDP-43 transcripts. Using species-specific quantitative real-time PCR we found that in one year old mutant mice endogenous mouse TDP-43 messenger RNA transcripts were decreased to as low as 20% compared to controls. In contrast, the human TDP-43 isoform carrying the A315T mutation was 3-fold upregulated (Fig. 1D). In summary, the ratio of hTDP-43$^{A315T}$ to mTDP-43 was calculated to be 15:1 as based on transcript levels.

**The 3'UTR is essential to control endogenous TDP-43 levels *in vivo***

TDP-43 regulates itself through a negative feedback loop by binding to its own 3'UTR sequence [17, 31]. This discovery led us to investigate if the missing 3'UTR in our construct was accountable for the hTDP-43 upregulation. We created four ES cell lines expressing either the human wildtype or mutant TDP-43 cDNA along with a bGH polyA sequence or 800bp of the mouse 3'UTR. Protein lysates of these clones were generated and analyzed. TDP-43 protein amounts of clones expressing either wildtype or mutant hTDP-43 together with the 3'UTR were comparable to the levels of the control. While the clones expressing the wildtype or mutant cDNA with the bGH polyA showed approximately 2.5-fold increase of TDP-43 protein (Fig. 2A). These experiments suggested that the elevated expression of human TDP-43 in the mutants was solely due to the absence of the 3' UTR. In addition, 800bp of the mouse 3'UTR were sufficient for the negative TDP-43 auto-loop. While performing a 3'RACE of mouse brain samples we detected two splice variants of the TDP-43 3'UTR of 828bp and 247bp (Fig. 2B). The spliced region contains a putative binding site for TDP-43 (red; Fig. 2C).

**Insoluble TDP-43 inclusions in hTDP-43$^{A315T}$ mice**

A pathological hallmark of amyotrophic lateral sclerosis (ALS) and frontotemporal lobar degeneration (FTLD-TDP) is the formation of neuronal insoluble TDP-43 inclusions [47, 48]. We detected insoluble TDP-43 in brain lysates of hTDP-43$^{A315T}$ +/- mice (Fig. 3A). The amount of insoluble TDP-43 protein increased with age: While three months old mice showed only small amounts of insoluble TDP-43, it became highly detectable in one year old mutants yet not in controls. This observation was made using an antibody detecting only the human TDP-43 (anti-hTDP-43) as well as using an antibody detecting both, human and mouse isoforms (anti-total TDP-43). Despite elevated expression of human TDP-43 being detected in all tissues tested, insoluble TDP-43 was only found in the brain yet not in the spleen, kidney or liver (Fig. 3B). Using immunhistochemistry we detected the presence of cytoplasmic TDP-43 aggregates in sections of brain and spinal cord of one year old hTDP-43$^{A315T}$ +/- mice with both, anti-hTDP-43 or anti-total TDP-43 antibodies (Fig. 3C). Neuronal cytoplasmic inclusions (NCIs) were present in the cortex and, to some extent, in hippocampal neurons. Furthermore, neurons in the anterior horn of the spinal cord exhibited TDP-43 aggregates and nuclear clearance. These findings support the view, that a mechanism leading to the formation of TDP-43 aggregates is only active in neurons.

**TDP-43 aggregates in brain and spinal cord of hTDP-43$^{A315T}$ mice**

A characteristic feature of neurodegenerative diseases is the ubiquitination of protein aggregates in the cytoplasm and/or nucleus of neurons [49]. Neumann et al. (2006) [47] were able to show that TDP-43 is the ubiquitinated protein in ALS and FTLD-TDP cases. To investigate possible ubiquitination of TDP-43 we performed double immunofluorescence labeling with antibodies recognizing both TDP-43 isoforms and poly-ubiquitin (Fig. 4A-D). TDP-43 (green) was shown to localize to the nucleus of neurons

of the brain and spinal cord in the control mice. The ubiquitin staining of the control sections (Fig. 4A,C) displayed a rather weak signal in comparison to sections from mutant mice (Fig. 4B,D). In the brain, the cortex and anterior horn of the spinal cord of mutants we detected TDP-43 inclusions in the cytoplasm of neurons that co-localized with ubiquitin (Fig. 4B,D). Another previously described pathological feature of TDP-43 in ALS and FTLD-TDP is hyperphosphorylation of the protein at several serine residues as well as the presence of a C-terminal 25kDa fragment [47]. To examine the phosphorylation status of TDP-43, we performed western blot analyses using soluble and insoluble brain protein fractions of 20 months old control and mutant mice. As positive control for a phospho-specific TDP-43 antibody we carried out *in vitro* phosphorylation of brain lysates using casein kinase I [50]. However, we were unable to detect hyperphosphorylation of TDP-43 in hTDP-43$^{A315T}$ animals. Also, disease-related C-terminal fragments of TDP-43 were not detected (not shown).

**Neurodegeneration in mice expressing human A315T TDP-43**

As ALS has been described as progressive neurodegenerative disease affecting upper and lower motor neurons, we analyzed the motor system of hTDP-43$^{A315T}$ +/- mice. In order to asses the number of motor neurons in the ventral horn of the spinal cord we performed Nissl staining of the lumbar spinal cord region in serial sections (Fig. 5A-B). Counting of neurons in the sciatic motor pool revealed that there was a 10% reduction of motor neurons compared to controls in 3 and 18 month old animals expressing the human A315T mutation (Fig. 5C), indicating a developmental phenotype. To test for a correlation between a decreased number of motor neurons and performance of the animals, several motor tests on a cohort of animals were done after 5 and 15 months. No abnormalities were seen in 5 months old animals (not shown). In the CatWalk analysis of the mutant animals an increase in gait abnormalities was determined, which was subtle yet significant as compared to control animals. Not only did hTDP-43$^{A315T}$ +/- mice spend more time standing on four paws compared to controls (Fig. 5D), the time at which the largest part of a paw contacted the glass plate was significantly altered for the left hind paws (Fig. 5E) and the temporal relationship of the diagonal inter-paw coordination was displaced in mutants (Fig. 5F). Other motor tests (ladder, accelerating rotarod, beam walk, grip strength and pole test) revealed no significant differences (Fig. 6). Patients suffering from ALS occasionally develop a form of dementia [51]. To this purpose we analyzed several memory tasks in one cohort of mice. The Y-maze, which is a test for working memory, showed a trend in female mutants towards unusually increased same arm returns (SARs) in comparison to aged-matched controls. Other memory tests including object recognition and IntelliCage no abnormalities could be detected in mutant mice (not shown). Summed up, these results suggest that the approx. 10% reduction of motor neurons observed is responsible for slight motoric problems.

**Changes in the metabolism of hTDP-43$^{A315T}$ mice**

Compared to both age and sex-matched controls, hTDP-43$^{A315T}$ +/- mice showed decreased body weight of 10% at an age of 15 months (Fig. 7A). In order to investigate this phenotype, we performed blood plasma sample analysis of six month old *ad libitum* fed and overnight fasted mice. While no significant genotype-related differences were observed for triglyceride levels of the *ad libitum* fed mice, glucose concentrations were slightly increased in both, male and female mutants of this group (Fig. 7B). Significant genotype-related differences were detected in blood lipid and glucose concentrations of overnight fasted mice, for which we determined decreased plasma cholesterol and triglyceride values (Fig. 7B). *Ad libitum* fed females showed increased ratio of HDL-cholesterol to total cholesterol, indicating a reduction of non-HDL cholesterol (Fig. 7C). In the intestine, triglycerides are broken

down to non-esterified fatty acids (NEFA), being the molecular species absorbed by enterocytes [52]. *Ad libitum* fed females showed increased NEFA concentrations in mutants (Fig. 7D) and plasma cholesterol levels were significantly increased in male mutants over male controls. Taken together, we observed a number of gender-specific changes in lipid content and a significant, loss of bodyweight of 10% in both sexes.

**TDP-43 regulates the expression of the PD related protein PARKIN and its target CD-36 negatively**

Mutations in the genes encoding *Progranulin* (GRN) and *Fus/Tls* are involved in sporadic and/or familiar forms of ALS or FTLD-TDP [53-56]. To examine the expression of these proteins we performed western blot analysis with brain lysates of 3 and 15 months old control and mutant animals. The expression levels of neither GRN nor FUS were affected by elevated hTDP-43$^{A315T}$ protein levels (not shown). Interestingly, the expression levels of the PD related protein Parkin were robustly reduced to approximately 30% of wildtype controls (Fig. 8A) at all ages, tested by real time PCR and western blotting. Parkin has previously been shown to be a potential TDP-43 target gene in iCLIP analysis [17]. Parkin also became connected to the process of mitophagy [57]. Hence, reduction of Parkin levels may be in agreement with accumulation of impaired mitochondria. For this reason, we analyzed protein levels of Optic atrophy 1 (OPA1), a protein controlling both mitochondrial fusion and cristae morphology [58]. We found an increase of OPA1 in young mutant animals indicating increased mitochondrial fusion. On the other hand, there was a shift towards more fragmentation of mitochondria in old mutants (Fig. 8B). Furthermore, Parkin has been brought in relation to the fat metabolism by regulating CD36 [59]. We therefore analyzed liver protein lysates of old and young hTDP-43$^{A315T}$ animals for CD36 protein levels. Interestingly, a significant reduction of CD36 levels of approximately 50% was determined in 15 month old mutants compared to controls (Fig. 8C). Collectively, these data suggest that elevated protein levels of hTDP-43$^{A315T}$ do not affect protein levels of FUS and GRN, while a clear negative effect in older animals on the PD related protein Parkin, the mitochondrial dynamin-related protein OPA1 and the fat metabolism associated protein CD36 is observed.

**Transcriptome analysis of brain and muscle**

Transcriptome analysis was performed for brain and muscle using 17 week old male mice, analyzing 4 to 6 biological replicates of each genotype group (in total 20 hybridizations). Statistical analysis of transcriptome profiles of the brain identified 50 differentially regulated genes in Tardbp mutant and control mice (Fig. 9). Ingenuity Pathways Analysis (IPA) based on 382 differentially expressed probes of microarray data from hTDP-43$^{A315T}$ mutants showed two significantly overrepresented biological functions: a. cell death (p-value=2.4x10$^{-4}$; including the regulated transcripts ATP6AP2, BCL2A1, BECN1, BMPR1B, CASP9, CD300LD, CDKN2C, EIF2AK4, EMD, ENO1, GPX4, IAPP, INSR, IRF1, MDM2, MSH2, RECQL, SF3B14, TGM2, TNFRSF25, UBE2K) as well as b. energy production / lipid metabolism (p-value=4.0x10$^{-3}$; incorporating AADAC, ECHS1, ESRRA, IAPP, INSR, LIPE, PPARGC1B, VDR; Fig. 10). In addition, a specific search for enriched GO categories with the same input data revealed the significantly overrepresented functions respiratory electron transport chain (p-value=6.8x10$^{-5}$; including ATP5F1, COX5A, NDUFA6, NDUFA8, NDUFS4, NDUFS7, SDHB) and mitochondria (p-value=3.2x10$^{-5}$; with regulated transcripts ACOT13, ATP5F1, AZI2, C6orf57, CASP9, COX5A, CYP11B2, DNAJC19, ECHS1, GCET2, GPX4, GTPBP8, HEMK1, HSH2D, IDH3B, IDH3G IVD, LOC100046650, MDH1, MLXIP, MPV17L, MRPL18, MRPL27, MRPL46, MRPL52, NDUFA6, NDUFA8, NDUFS4, NDUFS7, NLRX1, PPA2, RAB8B, SDHB, SIRT3, SLC25A16, SLC25A21, SRP19, TGM2, TIMM10, TIMM8B, WARS2).

Based on the results of the microarrays, we performed Transmission Electron Microscopy (TEM) of the motor cortex and hippocampus using 18 month old animals. Neuronal cells were identified by their surrounding myelin sheath. We showed that neurons of heterozygous hTDP-43$^{A315T}$ animals frequently displayed a mitochondrial dysmorphology with highly reduced cristae formation, which was not seen in wildtype littermates (Fig. 11). Abnormal cristae morphology was not observed in spinal cords (data not shown).

**Discussion**

An animal model of TDP-43 pathology with close resemblance to human disease could accelerate the development of drugs potentially slowing down disease progression. Mouse models expressing TDP-43 mutations *in trans* have often turned out unsatisfactory in this respect [1, 60]. Neither loss nor gain of function mutants could simultaneously recapitulate all the pathologic signs reported from ALS patients [47-48], such as progressive upper or lower motor neuron loss, skeletal muscle atrophy and paralysis, respiratory muscle failure, the presence of ubiquitinated and phosphorylated TDP-43 and C-terminal fragments [11-12, 35, 61-65]. The mutant forms of TDP-43 were not particularly aggregation-prone and the target spectrum of wildtype and mutant TDP-43 was apparently identical [66]. When overexpressed, the wildtype form of TDP-43 caused an even more severe phenotype than the mutant protein or C-terminal fragment [67-72]. ALS-like phenotypes observed in transgenic animals, had manifested already in younger mutants and, unlike the human condition, often resulted in early death [60, 73].

The RMCE mouse model of TDP-43 described in the present study for the first time provides *in vivo* evidence for mitochondrial dysmorphology and dysfunction as well as altered lipid metabolism, which may support an interpretation as a pre-disease model for a neurodegenerative disease. We show that the already suspected negative feedback loop of TDP-43 on its own transcription [17, 31] has significant *in vivo* relevance and we provide a minimal 3' RACE fragment of 800bp which was sufficient to exert negative regulation of TARDBP transcription (Fig. 2). When coupled to a bovine growth hormone polyA sequence, TDP-43 mRNA and protein levels were elevated up to 3-fold in total, although transcription of the non-affected allele was regulated down to only 20% of wildtype levels simultaneously (Fig. 1D). Hence, it is important to stress that this mouse is an overexpression model with more than 90% of all TDP-43 protein being the human A315T form. Downregulation of the wildtype allele indicated that the TDP-43 protein with the A315T point mutation was entirely functional with respect to its self-regulating ability. The mechanism of the negative auto-feedback of TDP-43 has been recently determined as self-splicing of the proximal polyA signal, which results in nuclear retention of the spliced transcript [74].

It has been well described that elevated TDP-43 protein levels can assert toxic effects on cells [33, 75]. A number of studies have reported elevated expression of TDP-43 in FTLD patients [76-79]. A strong argument in favour of the importance of the 3'UTR in humans was the discovery by Gitcho et al. (2009) [80] of an FTLD-MND patient, carrying a 3'UTR point mutation. TDP-43 levels were increased twofold in this case and the age of 66 years at disease-onset was earlier than in a patient carrying the A315T point mutation (83 years). We propose a model, in which the negative feedback loop of TDP-43 is critical for development of TDP-43 pathology: Once the TDP-43 protein is located in the cytoplasm, as a result of either TDP-43 protein modification, modified interaction partners or yet unidentified cellular stressors, the feedback loop in the nucleus will instantly cause an overshooting of TDP-43 protein levels. An excess of TDP-43 protein should be removed by ubiquitination with subsequent proteasomal activity. However, with continuous stress, the cellular proteasome is outnumbered by protein production which then results in cytoplasmic inclusions of ubiquitinated TDP-43. As we show, elevated levels

of TDP-43 (A315T) do not necessarily lead to the formation of insoluble protein. Although TDP-43 protein levels were high in all tissues tested, we were unable to detect insoluble protein in tissues other than the brain and spinal cord (Fig. 2). This indicates, that a yet unidentified mechanism exists, which promotes insolubility of TDP-43 in neuronal tissues. The pathway analysis of microarray data from hTDP-43$^{A315T}$ transgenic knock-in animals showed that clusters of regulated transcripts are either involved in cell death, energy production, respiratory electron chain, mitochondrial function or lipid metabolism (Fig. 10). On a hTDP-43$^{A315T}$ overexpressing background, genes were mostly negatively regulated, with the exception of LIM homeobox protein 1 (Lhx1), Mannan-binding lectin serine peptidase 2 (Masp2) and Enolase 1 (Eno1; Fig. 9). Lim-1 has a developmental role in head formation [82], Masp2 is involved in the complement cascade [83] while Eno1 encodes for alpha enolase, which is a glycolytic enzyme, and for the myc-binding protein (Mbp1) [83].

We demonstrate that elevated levels of TDP-43 A315T protein resulted in an increase in glucose and cholesterol concentrations in the plasma of *ad libitum* fed animals, as well as increased non esterified fatty acid (NEFA) and decreased cholesterol and triglyceride levels in plasma of overnight fasted mice (Fig. 7). However, all cells are capable to metabolize NEFA by esterification to glycerol and in the blood, the major proportion of fatty acids is transported as lipoprotein-associated triglycerides. Fatty acids are released from triglycerides by lipolytic activity occurring as intra-vascular lipoprotein-lipolysis and intracellular lipolysis [84]. Although 80-90% of infused lipoprotein-associated triglycerides are usually turned into NEFA within 15 minutes, plasma NEFA levels increase only moderately due to a high turnover of free fatty acids [85]. Prolonged fasting of mice elevates lipolytic activity resulting in an almost two-fold increase of free fatty acids and glycerol in the plasma of overnight fasted mice [86]. Weight loss is a well-known phenomenon among ALS patients [87]. A high lipid content in the blood has been correlated with survival and a high lipid diet has been suggested as beneficial for many ALS cases [88].

hTDP-43$^{A315T}$ overexpressing mice were approximately 10% underweight in comparison to littermates at all ages (Fig. 7A). Measurements of bone density, lean mass and fat mass from each ten wild-type or mutant males and females indicated that this loss of body mass was not due to skeletal muscle atrophy, but partially due to reduced bone mineral density in females and mainly a result of reduced fat tissue. In average, mutant females showed a slightly elevated fat mass reduction from 5.4g in wild-type littermates to 2.0g (37%) while mutant males showed a reduction in fat mass from 7.82g to 6.56g (84%).

A rapid loss of fat mass, leading to death 9-18 days after induction was previously reported from conditional TDP-43 mutant mice after crossbreeding with a widely expressed, tamoxifen-inducible Cre deleter strain [89]. The authors demonstrated a decrease in the expression of Tbc1d1 in mutant ES cells. Tbc1d1 is required for Glut4 translocation to the membrane of skeletal muscle cells and Glucose uptake [90] and is involved in human obesity [91-92]. We therefore examined Tbc1d1 protein levels in hTDP-43$^{A315T}$ mutants but did not detect any abnormalities in skeletal muscle or other tissues (not shown). The uptake of free fatty acids can be mediated in a large number of cells by the fatty acid transporter (FAT), also referred to as CD36. CD36 has been previously associated with insulin resistance [93] and atherosclerotic cardiovascular diseases [94]. We therefore analyzed the expression level of CD36 in hTDP-43$^{A315T}$ mutants and found a significant decrease of CD36 protein expression (Fig. 8C). A reduction of CD36 and thus a correlation with fat metabolism, has been recently reported from Parkin mutant animals [59]. Whether the relative reduction of Parkin detectable in hTDP-43$^{A315T}$ animals (Fig. 8A) was causing a decrease in CD36 is unclear. Parkin

was first identified as potential TDP-43 target gene by Polymenidou et al (2011) [17]. Parkin expression is usually induced in response to starvation and is elevated upon inhibition of mTOR signalling through rapamycin [95].

Motoric tests revealed normal grip strength of the mutants and only slight impairment of motor control (ladder, catwalk, rotarod, see Fig. 5D-F), which may also hint to yet undiscovered cerebellar dysfunction. However, when motor neurons of a 15 month old cohort of 5 mutants and 5 wildtypes were counted in a double-blinded fashion, a reduction of 10% was evident in the mutants (Fig. 5C). We questioned, whether this was a developmental defect or a progressive phenotype and counted motor neurons also in 3 month old animals. As it turned out, the 10% reduction of motor neurons could be already observed in younger animals, indicating a developmental phenotype which did not worsen with age (Fig. 5C). These results likely illustrate the vulnerability of motor neurons to high TDP-43 expression levels and may be unrelated to the A315T mutation. However, a similar construct with a hTDP-43 wild-type cDNA was not transmitted through the germline and direct comparisons were therefore not possible.

Transcriptome analysis followed by IPA and TEM revealed mitochondrial dysfunction in the brain (IPA) and frequent mitochondrial dysmorphology in the motor cortex (TEM) of hTDP-43$^{A315T}$ transgenic knock-in animals (Figs. 9 and 10). Mitochondrial abnormalities were also reported from a mouse model, that overexpressed human wild-type TDP-43 in the developing forebrain conditionally. They were however not observed after delayed overexpression in adult animals and were therefore considered developmental abnormalities [96]. Whether mitochondrial abnormality could explain the observed metabolic changes and altered body weight composition of hTDP-43$^{A315T}$ animals will be subject of future studies.

**Summary and outlook**

With respect to the fact that patients carrying A315T mutations develop either ALS or MND [80, 97] and a patient carrying a 3'UTR mutation of TDP-43 leading to overexpression of the protein developed FTLD, the mouse model presented here is interpreted as a pre-disease model for FTLD-MND. In agreement with this interpretation, TARDBP$^{KIA315T}$ animals showed slight gait and cognitive abnormalities along with a decrease in number of motor neurons but did not show primary motor phenotypes or muscular atrophy. We therefore believe that the animals could be invaluable in identifying environmental or genetic triggers that finally lead to full-blown FTLD or ALS.

**Acknowledgements**

We thank Helga Weichsberger, Sandra Geißler, Denise Herold and Irina Rodionova, Elfie Holupirek, Susanne Wittich, Anja Wohlbier, and Reinhard Seeliger for technical assistance. We are grateful to Anja Capell and Christian Haass for a Progranulin antibody. We would like to thank Constantin Stautner and Jordi Guimera for critical reading of the manuscript. This work was funded by the KNDD2 grants FKZ 01 GI 1005D to T.F. This work was also funded by the program for medical genome research with financial support from the Federal Ministry for Education and Research (BMBF) grant "Funktionelle Tiermodelle für die Kandidatengene der Alzheimerschen Erkrankung" (01GS08133), the grant "Verhalten" 01GS0850, furthermore by the Helmholtz Alliance “Mental Health in an Ageing Society” (HELMA) (HA215). This work supported by the Cluster of Excellence Frankfurt Macromolecular Complexes at the Goethe University Frankfurt DFG project EXC 115 (AR and SK). This study was supported in part by a grant from the German Federal Ministry of Education and Research (BMBF) to the German Center for Diabetes Research (DZD e.V.). The GMC was supported by NGFNplus (01GS0850) and Infrafrontier (01KX1012) grants from the BMBF and the EU (EUMODIC LSHG-2006-037188). This work was supported by grants to JB from the National Genome Research Network (NGFN 01GR). This project was supported by funds from the German

Federal Ministry of Education and Research (German Center for Vertigo and Balance Disorders, grant 01 EO 0901).

**Author Contributions**

T.F. designed the experiments. C.S. established the animals and performed all molecular analyses, A.S analyzed the impact of different 3'UTRs, B.R., W.H. and J.R. performed clinical biochemistry screens and metabolic analyses, M.H. and J.B. did microarrays, S.K. and A.R. looked for mitochondrial marker expression, L.G. and S.M.H did the behavioral analysis, M.A. and A.K.W. performed TEM, D.T. and R.A. did the bioinformatics, M.N. provided the patient cDNA, E.K. provided antibodies, H.F., V.G-D., M.H.D.A., E.W., M.K., T.K., L.B. ,W.W. and T.F. analyzed GMC data, F.N. advised in TDP-43 pathology, T.F. and C.S. analyzed the data and wrote the manuscript.

**Conflict of Interest**

The authors declare no conflicts of interest.

**References**

1. Rademakers R, Neumann M, Mackenzie IR (2012) Advances in understanding the molecular basis of frontotemporal dementia. Nat Rev Neurol 8: 423-434.
2. Andersen PM, Al-Chalabi A (2011) Clinical genetics of amyotrophic lateral sclerosis: what do we really know? Nat Rev Neurol 7: 603-615.
3. Janssens J, Kleinberger G, Wils H, Van Broeckhoven C (2011) The role of mutant TAR DNA-binding protein 43 in amyotrophic lateral sclerosis and frontotemporal lobar degeneration. Biochem Soc Trans 39: 954-959.
4. Bonini NM, Gitler AD (2011) Model organisms reveal insight into human neurodegenerative disease: ataxin-2 intermediate-length polyglutamine expansions are a risk factor for ALS. *J* Mol Neurosci 45: 676-683.
5. Wilson AC, Dugger BN, Dickson DW, Wang DS (2011) TDP-43 in aging and Alzheimer's disease - a review. Int J Clin Exp Pathol 4: 147-155.
6. Jucker M, Walker LC (2011) Pathogenic protein seeding in Alzheimer disease and other neurodegenerative disorders. Ann Neurol 70: 532-540.
7. Herman AM, Khandelwal PJ, Stanczyk BB, Rebeck GW, Moussa CE (2011) β-amyloid triggers ALS-associated TDP-43 pathology in AD models. Brain Res 22: 191-199.
8. Jellinger KA (2008) Neuropathological aspects of Alzheimer disease, Parkinson disease and frontotemporal dementia. Neurodegener Dis 5: 118-121.
9. Wang HY, Wang IF, Bose J, Shen CK (2004) Structural diversity and functional implications of the eukaryotic TDP gene family. Genomics 83: 130-139.
10. Colombrita C, Zennaro E, Fallini C, Weber M, Sommacal A et al (2009) TDP-43 is recruited to stress granules in conditions of oxidative insult. J Neurochem 111: 1051-1061.
11. Sephton CF, Good SK, Atkin S, Dewey CM, Mayer P 3rd et al (2010) TDP-43 is a developmentally regulated protein essential for early embryonic development. J Biol Chem 285: 6826-6834.
12. Wu LS, Cheng WC, Hou SC, Yan YT, Jiang ST et al (2010) TDP-43, a neuro-pathosignature factor, is essential for early mouse embryogenesis. Genesis 48: 56-62.
13. Chen-Plotkin AS, Lee VM, Trojanowski JQ (2010) TAR DNA-binding protein 43 in neurodegenerative disease. Nat Rev Neurol 6: 211-220.
14. Turner BJ, Bäumer D, Parkinson NJ, Scaber J, Ansorge O et al (2008)
15. TDP-43 expression in mouse models of amyotrophic lateral sclerosis and spinal muscular atrophy. BMC Neurosci 9: 104.

16. Ayala YM, Zago P, D'Ambrogio A, Xu YF, Petrucelli L et al (2008) Structural determinants of the cellular localization and shuttling of TDP-43. J Cell Sci 121: 3778-3785.
17. Kawahara Y, Mieda-Sato A (2012) TDP-43 promotes microRNA biogenesis as a component of the Drosha and Dicer complexes. Proc Natl Acad Sci U S A 109: 3347-3352.
18. Polymenidou M, Lagier-Tourenne C, Hutt KR, Huelga SC, Moran J et al (2011) Long pre-mRNA depletion and RNA missplicing contribute to neuronal vulnerability from loss of TDP-43. Nat Neurosci 14: 459-468.
19. Tollervey JR, Curk T, Rogelj B, Briese M, Cereda M et al (2011) Characterizing the RNA targets and position-dependent splicing regulation by TDP-43. Nat Neurosci 14: 452-458.
20. Xiao S, Sanelli T, Dib S, Sheps D, Findlater J et al (2011) RNA targets of TDP-43 identified by UV-CLIP are deregulated in ALS. Mol Cell Neurosci 47: 167-180.
21. Sephton CF, Cenik C, Kucukural A, Dammer EB, Cenik B et al (2011) Identification of neuronal RNA targets of TDP-43-containing ribonucleoprotein complexes. J Biol Chem 286: 1204-1215.
22. Buratti E, Baralle FE (2008) Multiple roles of TDP-43 in gene expression, splicing regulation, and human disease. Front Biosci 13: 867-878.
23. Polymenidou M, Lagier-Tourenne C, Hutt KR, Bennett CF, Cleveland DW et al (2012) Misregulated RNA processing in amyotrophic lateral sclerosis. Brain Res 1462: 3-15.
24. Liu-Yesucevitz L, Bilgutay A, Zhang YJ, Vanderweyde T, Citro A et al (2010) Tar DNA binding protein-43 (TDP-43) associates with stress granules: analysis of cultured cells and pathological brain tissue. PLoS One 5: e13250.
25. Dewey CM, Cenik B, Sephton CF, Dries DR, Mayer P 3rd et al (2011) TDP-43 is directed to stress granules by sorbitol, a novel physiological osmotic and oxidative stressor. Mol Cell Biol 31: 1098-1108.
26. Dewey CM, Cenik B, Sephton CF, Johnson BA, Herz J et al (2012) TDP-43 aggregation in neurodegeneration: Are stress granules the key? Brain Res 1462: 16-25
27. Gendron TF, Josephs KA, Petrucelli L (2010) Review: transactive response DNA-binding protein 43 (TDP-43): mechanisms of neurodegeneration. Neuropathol Appl Neurobiol 36: 97-112.
28. Ticozzi N, Ratti A, Silani V (2010) Protein aggregation and defective RNA metabolism as mechanisms for motor neuron damage. CNS Neurol Disord Drug Targets 9: 285-296.
29. Kuo PH, Doudeva LG, Wang YT, Shen CK, Yuan HS (2009) Structural insights into TDP-43 in nucleic-acid binding and domain interactions. Nucleic Acids Res 37: 1799-1808.
30. Wang IF, Chang HY, Hou SC, Liou GG, Way TD et al (2012) The self-interaction of native TDP-43 C terminus inhibits its degradation and contributes to early proteinopathies. Nat Commun 3: 766.
31. Freibaum BD, Chitta RK, High AA, Taylor JP (2010) Global analysis of TDP-43 interacting proteins reveals strong association with RNA splicing and translation machinery. J Proteome Res 9: 1104-1120.
32. Ayala YM, De Conti L, Avendaño-Vázquez SE, Dhir A, Romano M et al (2011) TDP-43 regulates its mRNA levels through a negative feedback loop. EMBO J 30: 277-288.
33. Budini M, Buratti E (2011) TDP-43 autoregulation: implications for disease. J Mol Neurosci 45: 473-479.
34. Johnson BS, Snead D, Lee JJ, McCaffery JM, Shorter J, Gitler AD

(2009) TDP-43 is intrinsically aggregation-prone, and amyotrophic lateral sclerosis-linked mutations accelerate aggregation and increase toxicity. J Biol Chem 284: 20329-20339.
35. Estes PS, Boehringer A, Zwick R, Tang JE, Grigsby B et al (2011) Wild-type and A315T mutant TDP-43 exert differential neurotoxicity in a Drosophila model of ALS. Hum Mol Genet 20: 2308-2321.
36. Wegorzewska I, Bell S, Cairns NJ, Miller TM, Baloh RH (2009) TDP-43 mutant transgenic mice develop features of ALS and frontotemporal lobar degeneration. Proc Natl Acad Sci U S A 106: 18809-18814.
37. Wang Q, Zhang X, Chen S, Zhang X, Zhang S et al (2011) Prevention of motor neuron degeneration by novel iron chelators in SOD1(G93A) transgenic mice of amyotrophic lateral sclerosis. Neurodegener Dis 8: 310-321.
38. Dance A (2010) TDP-43 models coverage. J Alzheimers Dis 21: 1403-1408.
39. Schebelle L, Wolf C, Stribl C, Javaheri T, Schnütgen F et al (2010) Efficient conditional and promoter-specific in vivo expression of cDNAs of choice by taking advantage of recombinase-mediated cassette exchange using FlEx gene traps. Nucleic Acids Res 38: e106.
40. Neumann M, Kwong LK, Lee EB, Kremmer E, Flatley A et al (2009) Phosphorylation of S409/410 of TDP-43 is a consistent feature in all sporadic and familial forms of TDP-43 proteinopathies. Acta Neuropathol 117: 137-149.
41. Li M, Pevny L, Lovell-Badge R, Smith A (1998) Generation of purified neural precursors from embryonic stem cells by lineage selection. Curr Biol 8: 971-974.
42. Hill PD, Wurst W (1993) Screening of novel pattern formation of genes using gene trap approaches. Methods in Enzymology 225: 664–681.
43. Hölter SM, Mandillo S, Tucci V, Nolan PM, Meziane H et al (2008) Reliability, Robustness and Reproducibility in mouse behavioral phenotyping: a cross-laboratory study. Physiol Genomics 34: 243-255.
44. Hölter SM, Glasl L (2011) High throughput mouse phenotyping. In: Dunnett SB, Lane E, (ed) Animal models of movement disorders, Human Press, New York, pp 109-133.
45. Zhou X, Tuck DP (2007) MSVM-RFE: extensions of SVM-RFE for multiclass gene selection on DNA microarray data. Bioinformatics 23(9): 1106-1114.
46. Augustin R, Lichtenthaler SF, Greeff M, Hansen J, Wurst W et al (2011) Bioinformatics identification of modules of transcription factor binding sites in Alzheimer's disease-related genes by in silico promoter analysis and microarrays. Int J Alzheimers Dis 2011: 154325.
47. Ashburner M, Ball CA, Blake JA, Botstein D, Butler H et al (2000) Gene ontology: tool for the unification of biology. The Gene Ontology Consortium. Nat Genet 25: 25-29.
48. Neumann M, Sampathu DM, Kwong LK, Truax AC, Micsenyi MC et al (2006) Ubiquitinated TDP-43 in frontotemporal lobar degeneration and amyotrophic lateral sclerosis. Science 314: 130-133.
49. Arai T, Hasegawa M, Akiyama H, Ikeda K, Nonaka T et al (2006) TDP-43 is a component of ubiquitin-positive tau-negative inclusions in frontotemporal lobar degeneration and amyotrophic lateral sclerosis. Biochem Biophys Res Commun 351: 602-611.
50. Forman MS, Trojanowski JQ, Lee VM (2004) Neurodegenerative diseases: a decade of discoveries paves the way for therapeutic breakthroughs. Nat Med 10: 1055-1063.

51. Kametani F, Nonaka T, Suzuki T, Arai T, Dohmae N et al (2009) Identification of casein kinase-1 phosphorylation sites on TDP-43. Biochem Biophys Res Commun 382: 405-409.
52. Lillo P, Hodges JR (2009) Frontotemporal dementia and motor neurone disease: overlapping clinicpathological disorders. J Clin Neurosci 16: 1131-1135.
53. Fergani A, Oudart H, Gonzalez De Aguilar JL, Fricker B, René F et al (2007) Increased peripheral lipid clearance in an animal model of amyotrophic lateral sclerosis. J Lipid Res 48: 1571-1580.
54. Baker M, Mackenzie IR, Pickering-Brown SM, Gass J, Rademakers R et al (2006) Mutations in progranulin cause tau-negative frontotemporal dementia linked to chromosome 17. Nature 442: 916-919.
55. Cruts M, Gijselinck I, van der Zee J, Engelborghs S, Wils H et al (2006) Null mutations in progranulin cause ubiquitin-positive frontotemporal dementia linked to chromosome 17q21. Nature 442: 920-924.
56. Kwiatkowski TJ, Bosco DA, Leclerc AL, Tamrazian E, Vanderburg CR et al (2009) Mutations in the FUS/TLS gene on chromosome 16 cause familial amyotrophic lateral sclerosis. Science 323: 1205–1208.
57. Vance C, Rogelj B, Hortobágyi T, De Vos KJ, Nishimura AL et al (2009) Mutations in FUS, an RNA processing protein, cause familial amyotrophic lateral sclerosis type 6. Science 323: 1208–1211.
58. Narendra D, Tanaka A, Suen DF, Youle RJ (2008) Parkin is recruited selectively to impaired mitochondria and promotes their autophagy. J Cell Biol 183: 795–803
59. Hoppins S, Lackner L, Nunnari J (2007) The machines that divide and fuse mitochondria. Annu. Rev. Biochem 76: 751-780.
60. Kim KY, Stevens MV, Akter MH, Rusk SE, Huang RJ et al (2011) Parkin is a lipid-responsive regulator of fat uptake in mice and mutant human cells. J Clin Invest 121: 3701-3712.
61. Tsao W, Jeong YH, Lin S, Ling J, Price DL et al (2012) Rodent models of TDP-43: Recent advances. Brain Res 1462: 26-39.
62. Wils H, Kleinberger G, Janssens J, Pereson S, Joris G et al (2010) TDP-43 transgenic mice develop spastic paralysis and neuronal inclusions characteristic of ALS and frontotemporal lobar degeneration. Proc Natl Acad Sci U S A 107: 3858-3863.
63. Igaz LM, Kwong LK, Lee EB, Chen-Plotkin A, Swanson E et al (2011) Dysregulation of the ALS-associated gene TDP-43 leads to neuronal death and degeneration in mice. J Clin Invest 121: 726-738.
64. Huang C, Tong J, Bi F, Zhou H, Xia XG (2012) Mutant TDP-43 in motor neurons promotes the onset and progression of ALS in rats. J Clin Invest 122: 107-118.
65. Kabashi E, Lin L, Tradewell ML, Dion PA, Bercier V et al (2010) Gain and loss of function of ALS-related mutations of TARDBP (TDP-43) cause motor deficits kDa. Hum Mol Genet 19: 671-683.
66. Kraemer BC, Schuck T, Wheeler JM, Robinson LC, Trojanowski JQ et al (2010) Loss of murine TDP-43 disrupts motor function and plays an essential role in embryogenesis. Acta Neuropathol 119: 409-419.
67. Li Y, Ray P, Rao EJ, Shi C, Guo W et al (2010) A Drosophila model for TDP-43 proteinopathy. Proc Natl Acad Sci U S A 107: 3169-3174.
68. Caccamo A, Majumder S, Oddo S (2012) Cognitive decline typical of frontotemporal lobar degeneration in transgenic mice expressing the 25-kDa C-terminal fragment of TDP-43. Am J Pathol 180: 293-302.

69. Stallings NR, Puttaparthi K, Luther CM, Burns DK, Elliott JL (2010) Progressive motor weakness in transgenic mice expressing human TDP-43. Neurobiol Dis 40: 404-414.
70. Swarup V, Phaneuf D, Dupré N, Petri S, Strong M et al (2011) Deregulation of TDP-43 in amyotrophic lateral sclerosis triggers nuclear factor κB-mediated pathogenic pathways. J Exp Med 208: 2429-2447.
71. Tsai KJ, Yang CH, Fang YH, Cho KH, Chien WL et al (2010) Elevated expression of TDP-43 in the forebrain of mice is sufficient to cause neurological and pathological phenotypes mimicking FTLD-U. J Exp Med 207: 1661-1673.
72. Xu YF, Gendron TF, Zhang YJ, Lin WL, D'Alton S et al (2010) Wild-type human TDP-43 expression causes TDP-43 phosphorylation, mitochondrial aggregation, motor deficits, and early mortality in transgenic mice. J Neurosci 30: 10851-10859.
73. Zhang YJ, Gendron TF, Xu YF, Ko LW, Yen SH et al (2010) Phosphorylation regulates proteasomal-mediated degradation and solubility of TAR DNA binding protein-43 C-terminal fragments. Mol Neurodegener 5: 33.
74. Gendron TF, Petrucelli L (2011) Rodent models of TDP-43 proteinopathy: investigating the mechanisms of TDP-43-mediated neurodegeneration. J Mol Neurosci 45: 486-499.
75. Avendaño-Vázquez SE, Dhir A, Bembich S, Buratti E, Proudfoot N et al (2012) Autoregulation of TDP-43 mRNA levels involves interplay between transcription, splicing, and alternative polyA site selection. Genes Dev 26: 1679-1684.
76. Suzuki H, Matsuoka M (2012) TDP-43 toxicity is mediated by the unfolded protein response-unrelated induction of C/EBP homologous protein expression. J Neurosci Res 90: 641-647.
77. Mishra M, Paunesku T, Woloschak GE, Siddique T, Zhu LJ et al (2007) Gene expression analysis of frontotemporal lobar degeneration of the motor neuron disease type with ubiquitinated inclusions. Acta Neuropathol 114: 81-94.
78. Chen-Plotkin AS, Geser F, Plotkin JB, Clark CM, Kwong LK et al (2008) Variations in the progranulin gene affect global gene expression in frontotemporal lobar degeneration. Hum Mol Genet 17: 1349-1362.
79. Kabashi E, Valdmanis PN, Dion P, Spiegelman D, McConkey BJ et al (2008) TARDBP mutations in individuals with sporadic and familial amyotrophic lateral sclerosis. Nat Genet 40: 572-574.
80. Weihl CC, Temiz P, Miller SE, Watts G, Smith C et al (2008) TDP-43 accumulation in inclusion body myopathy muscle suggests a common pathogenic mechanism with frontotemporal dementia. J Neurol Neurosurg Psychiatry 79: 1186-1189.
81. Gitcho MA, Bigio EH, Mishra M, Johnson N, Weintraub S et al (2009) TARDBP 3'-UTR variant in autopsy-confirmed frontotemporal lobar degeneration with TDP-43 proteinopathy. Acta Neuropathol 118: 633-645.
82. Takahashi M, Mori S, Shigeta S, Fujita T (2007) Role of MBL-associated serine protease (MASP) on activation of the lectin complement pathway. Adv Exp Med Biol 598: 93-104.
83. Shawlot W, Behringer RR (1995). "Requirement for Lim1 in head-organizer function.". *Nature* **374** (6521): 425–30.
84. Subramanian A, Miller DM (2000) Structural analysis of alpha-enolase. Mapping the functional domains involved in down-regulation of the c-

myc protooncogene. J Biol Chem 275: 5958-5965.
85. Zechner R, Zimmermann R, Eichmann TO, Kohlwein SD, Haemmerle G et al (2012) FAT SIGNALS-lipases and lipolysis in lipid metabolism and signaling. Cell Metab 15: 279-291
86. Teusink B, Voshol PJ, Dahlmans VE, Rensen PC, Pijl H et al (2003) Contribution of fatty acids released from lipolysis of plasma triglycerides to total plasma fatty acid flux and tissue-specific fatty acid uptake. Diabetes 52: 614-620.
87. Kersten S, Seydoux J, Peters JM, Gonzalez FJ, Desvergne B et al (1999) Peroxisome proliferator-activated receptor alpha mediates the adaptive response to fasting. J Clin Invest 103:1489-1498.
88. Dupuis L, Oudart H, René F, Gonzalez de Aguilar JL, Loeffler JP (2004) Evidence for defective energy homeostasis in amyotrophic lateral sclerosis: benefit of a high-energy diet in a transgenic mouse model. Proc Natl Acad Sci USA 101: 11159-11164.
89. Dorst J, Kühnlein P, Hendrich C, Kassubek J, Sperfeld AD et al (2011) Patients with elevated triglyceride and cholesterol serum levels have a prolonged survival in amyotrophic lateral sclerosis. J Neurol 258: 613-617.
90. Chiang PM, Ling J, Jeong YH, Price DL, Aja SM et al (2010) Deletion of TDP-43 down-regulates Tbc1d1, a gene linked to obesity, and alters body fat metabolism. Proc Natl Acad Sci U S A 107: 16320-16324.
91. Chadt A, Leicht K, Deshmukh A, Jiang LQ, Scherneck S et al (2008) Tbc1d1 mutation in lean mouse strain confers leanness and protects from diet-induced obesity. Nat Genet 40: 1354-1359.
92. Meyre D, Farge M, Lecoeur C, Proenca C, Durand E et al (2008) R125W coding variant in TBC1D1 confers risk for familial obesity and contributes to linkage on chromosome 4p14 in the French population. Hum Mol Genet 17: 1798-1802.
93. Stone S, Abkevich V, Russell DL, Riley R, Timms K et al (2006) TBC1D1 is a candidate for a severe obesity gene and evidence for a gene/gene interaction in obesity predisposition. Hum Mol Genet 15: 2709-2720.
94. Miyaoka K, Kuwasako T, Hirano K, Nozaki S, Yamashita S et al (2001) CD36 deficiency associated with insulin resistance. Lancet 357: 686-687.
95. Hirano K, Kuwasako T, Nakagawa-Toyama Y, Janabi M, Yamashita S et al (2003) Pathophysiology of human genetic CD36 deficiency. Trends Cardiovasc Med 13: 136-141.
96. Klinkenberg M, Gispert S, Dominguez-Bautista JA, Braun I, Auburger G et al (2012) Restriction of trophic factors and nutrients induces PARKIN expression. Neurogenetics 13: 9-21.
97. Cannon A, Yang B, Knight J, Farnham IM, Zhang Y, Wuertzer CA, D'Alton S, Lin WL, Castane-des-Casey M, Rousseau L, Scott B, Jurasic M, Howard J, Yu X, Bailey R, Sarkisian MR, Dickson DW, Petrucelli L, Lewis J. (2012): Neuronal sensitivity to TDP-43 overexpression is dependent on timing of induction. Acta Neuropathol. 123(6):807-23.
98. Gitcho MA, Baloh RH, Chakraverty S, Mayo K, Norton JB et al (2008) TDP-43 A315T mutation in familial motor neuron disease. Ann Neurol 63: 535-538.

**Figure legends**

**Fig. 1**
TDP-43 expression in heterozygous hTDP43A315T mice. (A) Homozygous animals expressing human A315T TDP-43 were embryonic lethal at weaning age. Agarose gel: At stage E7.5 no homozygous embryo was found. (B) Western blots of various tissue lysates from a 6 months old mutant mouse compared to control probed for total TDP-43 or human TDP-43 revealed tissue-specific pattern as well as increased TDP-43 levels for all organs. (C) Western blots of brain lysates from 1,6, and 12 months old mutants (+/-) and controls (wt) using antibodies against total TDP-43 and human TDP-43. (D) Quantification of mouse and human TDP-43 isoforms via quantitative real-time PCR. Down-regulation of endogenous mouse TDP-43 to about 20% as well as a 3 to 4 fold up-regulation of human TDP-43 in mutants compared to controls.

**Fig. 2**
The 3'UTR is essential to control endogenous TDP-43 levels. (A) Western blot of ES cells expressing either human wildtype TDP-43 with Bgh polyA, human A315T TDP-43 with Bgh polyA, human wildtpye and human A315T TDP-43 with 3'UTR under control of the endogenous TDP-43 promoter. Cells expressing human wildtype TDP-43 with bgh polyA showed 3-fold increased TDP-43 levels compared to untransfected control. Cells expressing human wildtype or mutant TDP-43 with 3'UTR display similar levels as control. (B) 3'RACE of the TDP-43 3'UTR revealed different splicing variants. (C) Spliced sequence within the 3'UTR.

**Fig. 3**
Insoluble TDP-43 in mutant mice. (A) Western blots of brain lysates from control (ctrl) and heterozygous (+/-) mutant mice using total TDP-43 and human specific TDP-43 antibodies at 3 and 12 months showed that mutant mice developed insoluble TDP-43 that increase with age. (B) Western blots of various tissues display insoluble TDP-43 in brain lysates but not in other tissues. (C) Immunohistochemistry of brain and spinal cord sections using human TDP-43 and total TDP-43 antibody revealed cytoplasmic TDP-43 inclusions (arrows) in the cortex and the ventral horn of the spinal cord at 12 months. Normal nuclear staining (arrowheads) of neurons was also detectable.

**Fig. 4**
Ubiquitin pathology in brains and spinal cords of one year old mutant mice. (A-D) Co-labeling of ubiquitin aggregates with total TDP-43 antibody revealing co-aggregation of ubiquitin and TDP-43 in the cytoplasm of brain (B) and spinal cord (D) (white arrows). Co-aggregation was not seen in brain (A) and spinal cord (C) sections of control mice.

**Fig. 5**
Nissl staining of the lumbar spinal cord region in serial sections (A,B). Counting of neurons in the sciatic motor pool (C). (D-F) Gait analysis. Mutant mice spent more time standing on four paws (D). Time at which the largest part of a paw contacted the glass plate was significantly altered for the left hind paws of mutants (E). The temporal relationship of the diagonal inter-paw coordination was displaced in mutants (F).

**Fig.6**
Behavioral analysis of mutant mice. There were few significant differences in the motor tests of 5 and 15 months old mutant mice compared to age matched controls. Only 5 months old females had more slips on the ladder and both 5 and 15 months old animals showed slight abnormalities in the gait analysis (CatWalk). 15 months old female mutants displayed longer turning duration on top of the pole, which was not yet significant. In all memory tests mutants behaved compara-

ble to controls. Again females showed a trend for same arm returns (SARs) in the Y-maze (trend = t-test, $0.1 > P < 0.05$; significant = t-test, $P < 0.05$).

**Fig.7**
Reduced body weight and changes in metabolism parameters in mutants. (A) Body weight changes were compared in male and female mutants. Both sexes show significantly reduced body weight as compared to controls. (B) Overnight fasted mutant mice displayed decreased cholesterol and triglycerides levels. No signifcant changes in glucose levels of overnight fasted and ad libitum fed mice. (C) The proportion of HDL-cholesterol on total cholesterol was increased in these mice. (D) Slightly increased NEFA concentrations in female mutant mice (* = t-test, $P < 0.05$; ** = t-test, $P < 0.01$; *** = t-test, $P < 0.001$).

**Fig.8**
Downstream targets of TDP-43. Western blot analysis of brain lysates from 3 and 15 months old mutants compared to controls showing decreased protein level for the Parkinson disease related protein Parkin (A) of about 70%. The autophagic marker Opa-1 was found to be elevated in 3 months old and decreased in 15 months old mutants (B). CD-36 protein was significantly reduced in old mutants as compared to controls (C).

**Fig.9**
Heat map of brain from gene expression profiling experiments Tardbp mutants versus control animals. The expression differences are represented by the fold changes = mutant/mean controls. The scale bar encodes the ratio of the fold induction. Blue/yellow color corresponds to transcriptional repression/induction in the mutant mice. The color intensity reflects the magnitude of the change gene expression levels on average.

**Fig.10**
IPA network Energy Production / Lipid Metabolism of regulated genes in brain of Tardbp mutant mice. Nodes with red colour represent upregulated whereas those with green colour downregulated transcripts from microarray data.

**Fig. 11**
Transmission electron micrographs of mitochondria of hippocampus and motor cortex. Mitochondria of myelinated neurons were compared between wt and heterozygotes. Hippocampus: Mitochondria of the hippocampus of heterozygous mice did not show any alterations in comparison to wt litermates (scale bar = 200 nm). Cortex: In the cortex of heterozygous mice, mitochondria appeared with a reduced number of cristae in comparison to wt litermates (scale bar = 200 nm).

**Figures**

Stribl_Fig.1

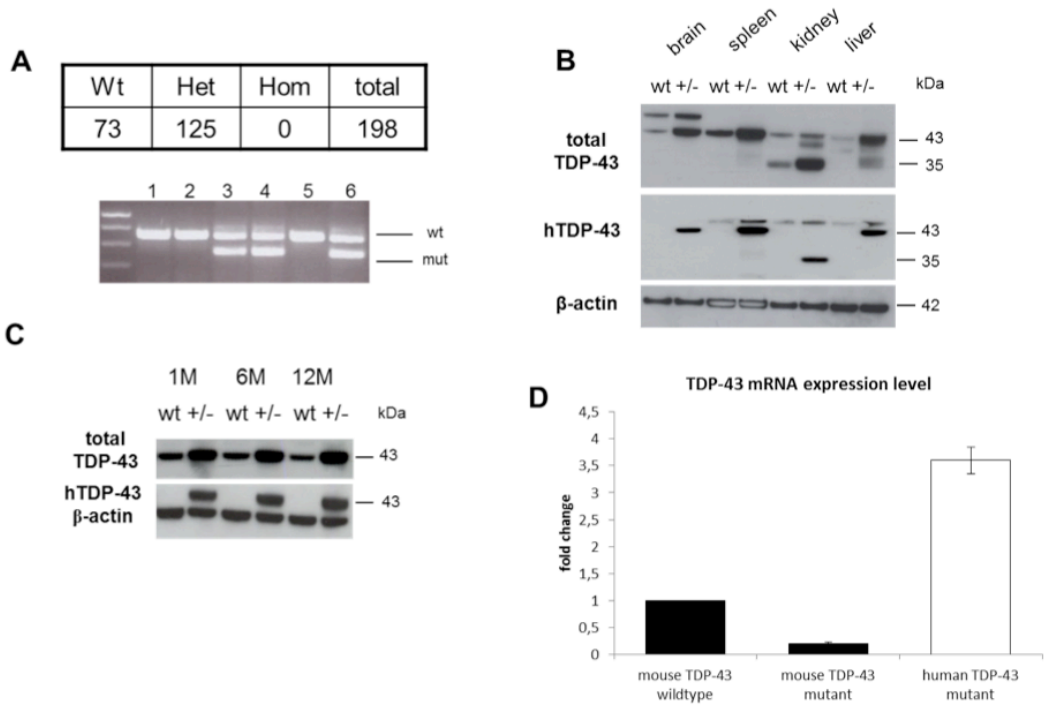

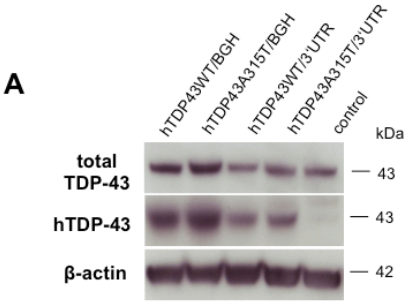


Stribl_Fig.2

C

GTGGGTGTTCCATTTTTATCCGCTACTCTTTATTTCATGGAGT
CGTATCAACGCTATGAACGCAAGGCTGTGATATGGAACCAGA
AGGCTGTTTGAACTTTTGAAACCTTGTGTGGGATTGATGGTG
GTGCCGAGGCATGAAAGGCTAGTATGAGCGAGAAAAGGAGA
GCGCGTGCAGAGACTTGGTGGTGGAAAATGGATATTTTTTAA
CTTGGAGAGATGTGTCACTCAATCCTGTGGCTTTGGTGAGA
GAGTGTGCAGAGAGCAATGATAGCAAATAACGTACGAATGTT
TTACATCAAAGGACATCCACATCAGTTGGAAGACTTTGAGTTT
TGTTCTTAGGAAACCCACTTTAGTTGAATGTGTTAAGTGAAAT
ACTTGTACTTCCCTCCCCCTCTGTCAACTGCTGTGAATGCTG
TATGGTGTGTGTTCTCCTCTGTTACTGATCTGGAAGTGTGGG
AACGTGAACTGAAGCTGATGGGCTGCGAACATGGACTGAGC
TTGTGGTGTGCTTTGCAGGAGAACTTGGAAGCAGAGTTCAC
CAGTGAGCTCAGGTGTCTCAAAGAAGGGTGGAAGTTCTCAT
GTCTGTTAGCTATTCATAAGAATGCTGTTTGCTGCAGTTCTGT
GTCCTGTGCTTGGATGCTTTTTTATAAGAGTTGTCATTGTTGG
AAATT

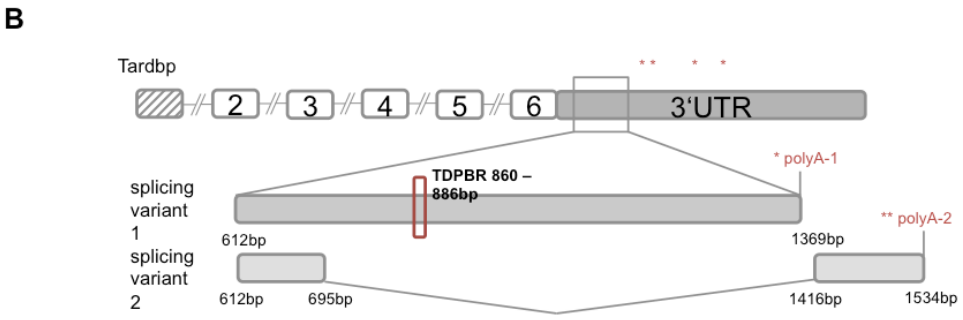

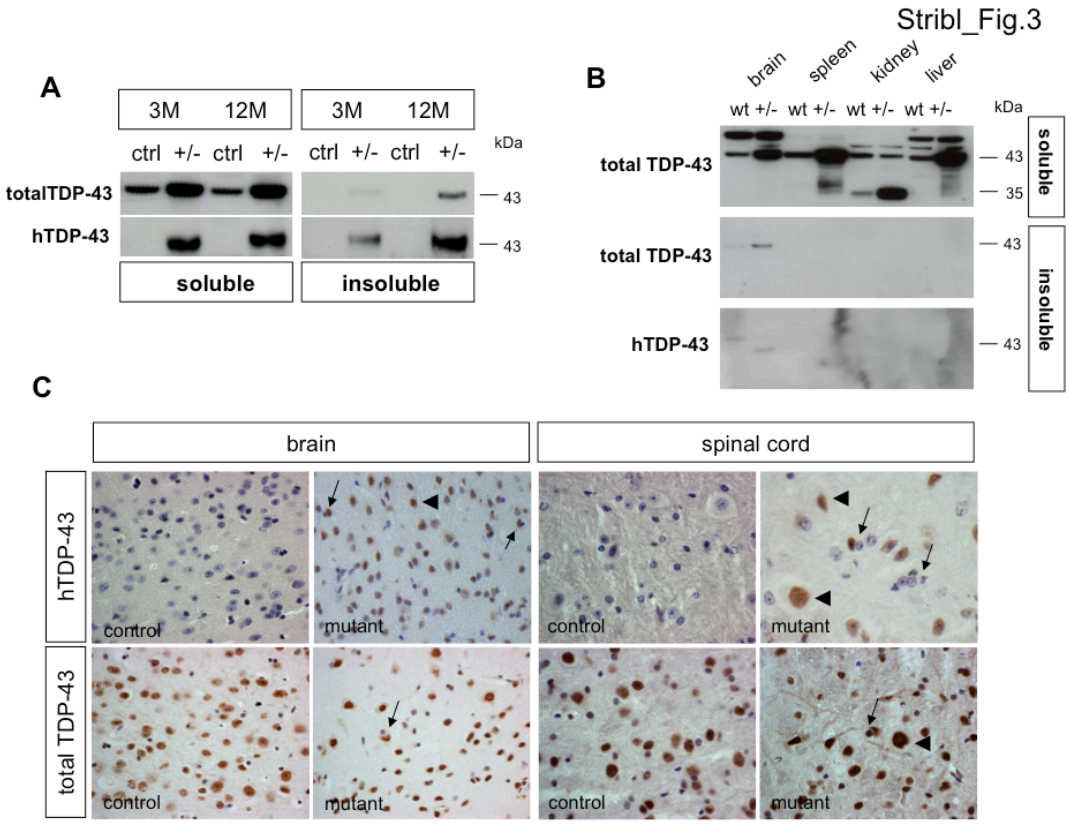

Stribl_Fig.4

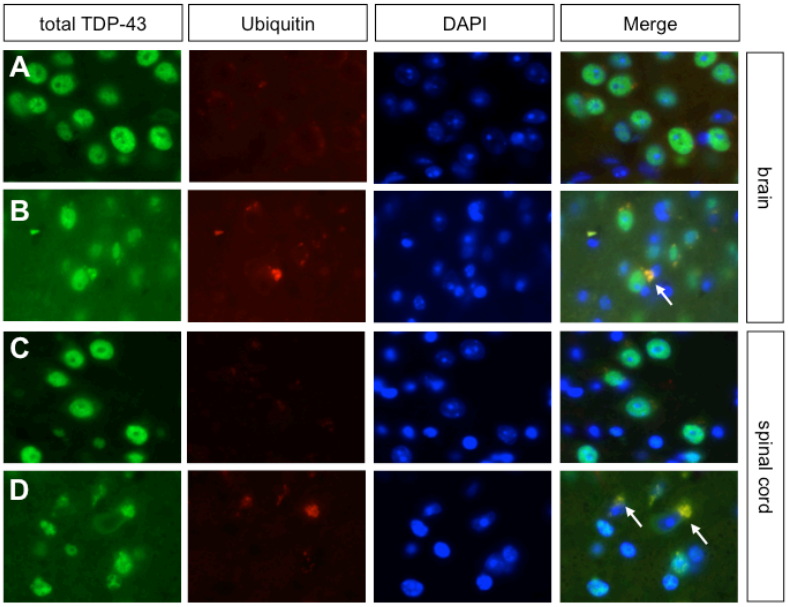

Stribl_Fig.5

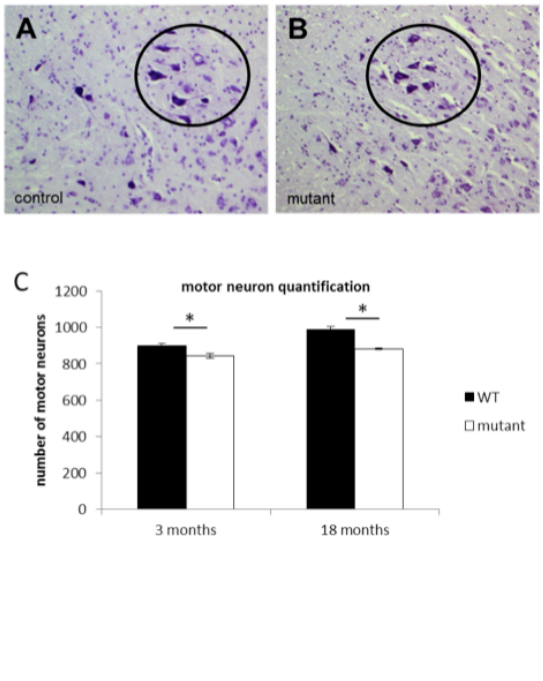

Stribl_Fig. 6

| | Test | female 5M | male 15 M | female 15 M |
|---|---|---|---|---|
| Motor tests | CatWalk | significant | significant | significant |
| | Beam walk | n.s. | n.s. | n.s. |
| | Pole test | n.s. | n.s. | trend (turning duration) |
| | Ladder | significant | n.s. | n.s. |
| | Rotarod | n.s. | n.s. | n.s. |
| | Grip strenght | n.s. | n.s. | n.s. |
| Memory tests | Y-Maze | n.d. | n.s. | trend (same arm return) |
| | Object recognition | n.d. | n.s. | n.s. |
| | IntelliCage | n.d. | n.d. | n.s. |

Stribl_Fig. 7

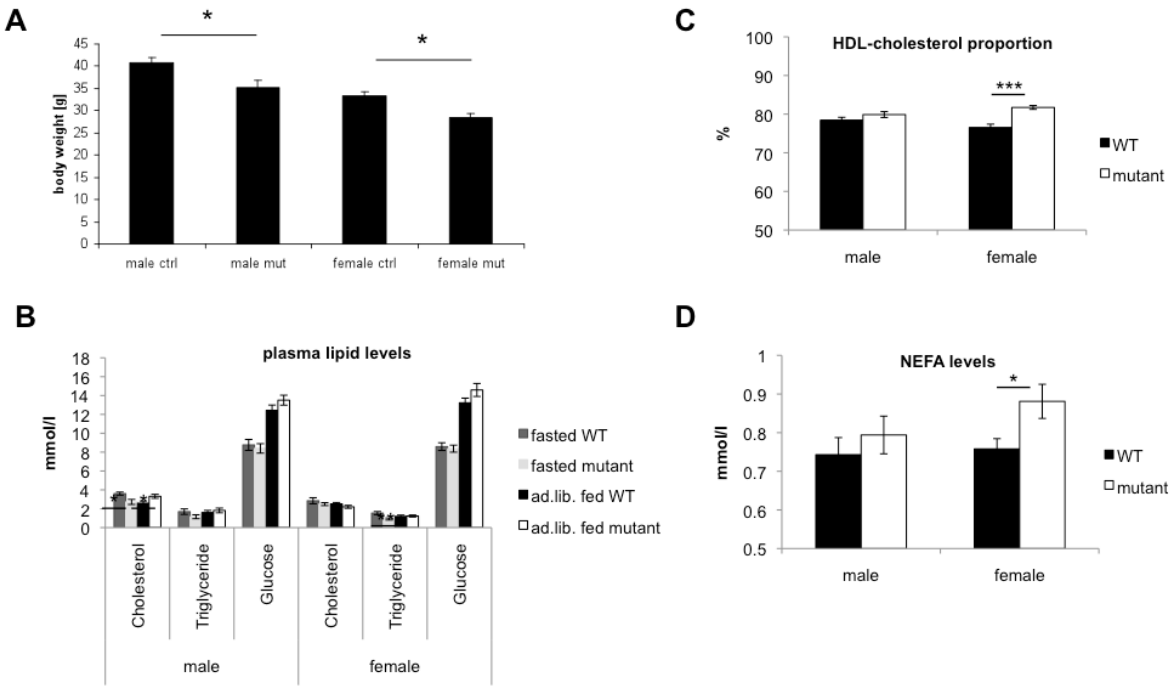

Stribl_Fig. 8

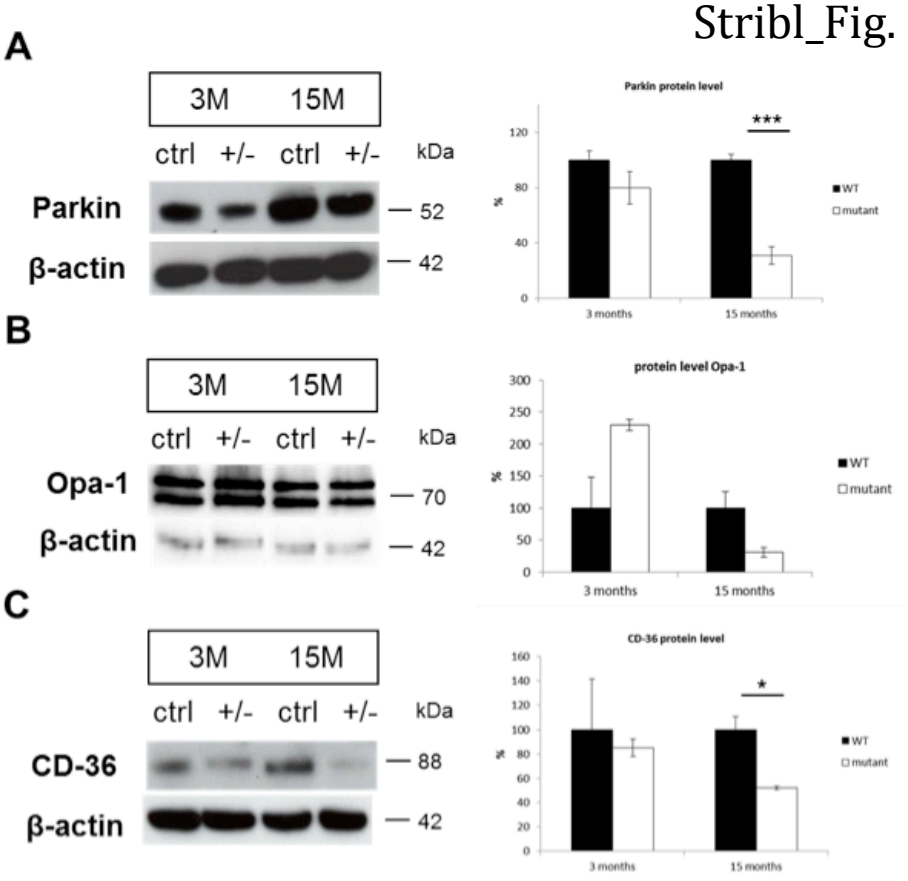

Stribl_Fig. 9


| Mean ratio | 464 505 511 543 549 | Gene symbol | Gene name |
|---|---|---|---|
| 2,06 | | Lhx1 | LIM homeobox protein 1 |
| 1,65 | | Eno1 | enolase 1, alpha |
| 2,62 | | Masp2 | mannan-binding lectin serine peptidase 2 |
| -5,38 | | Klk1b22 | kallikrein 1-related peptidase b22 |
| -2,47 | | Actc1 | actin, alpha |
| -2,94 | | Myl3 | myosin, light polypeptide 3 |
| -2,55 | | Mup1 | major urinary protein 1 |
| -2,39 | | Hoxb7 | homeobox B7 |
| -2,77 | | Myl2 | myosin, light polypeptide 2 |
| -2,60 | | Mup2 | major urinary protein 2 |
| -2,00 | | Vmo1 | vitelline membrane outer layer 1 |
| -1,65 | | Mylc2b | myosin, light chain 12B |
| -1,76 | | Cyp4a14 | cytochrome P450, family 4, subfamily a, polypeptide 14 |
| -1,94 | | Snx3 | sorting nexin 3 |
| -1,84 | | Tcfap2c | transcription factor AP-2, gamma |
| -1,57 | | Atg3 | autophagy-related 3 |
| -1,64 | | Dbt | dihydrolipoamide branched chain transacylase E2 |
| -1,69 | | Rab34 | RAB34, member of RAS oncogene family |
| -1,61 | | Mb | myoglobin |
| -1,63 | | Popdc2 | popeye domain containing 2 |
| -1,79 | | Clstn1 | calsyntenin 1 |
| -1,53 | | Clpx | caseinolytic peptidase X |
| -2,42 | | Hoxc6 | homeobox C6 |
| -1,50 | | Nhp2l1 | NHP2 non-histone chromosome protein 2-like 1 |
| -1,86 | | Mb | myoglobin |
| -1,50 | | Ccdc59 | coiled-coil domain containing 59 |
| -1,79 | | Olfr42 | olfactory receptor 263 |
| -2,15 | | Casp9 | caspase 9 |
| -1,86 | | Tcf20 | transcription factor 20 |
| -2,50 | | Cyp2a5 | cytochrome P450, family 2, subfamily a, polypeptide 5 |
| -1,47 | | Peg10 | paternally expressed 10 |
| -1,56 | | Vwa5a | von Willebrand factor A domain containing 5A |
| -1,83 | | Pik3r4 | phosphatidylinositol 3 kinase, regulatory subunit 4, p150 |
| -1,50 | | Tardbp | TAR DNA binding protein |
| -1,64 | | Atad2 | ATPase family, AAA domain containing 2 |
| -1,66 | | Polr2k | polymerase (RNA) II (DNA directed) polypeptide K |
| -2,13 | | Nppa | natriuretic peptide type A |
| -1,55 | | Ccdc53 | coiled-coil domain containing 53 |
| -1,67 | | H2-T23 | histocompatibility 2, T region locus 23 |
| -1,74 | | Atp13a5 | ATPase type 13A5 |
| -1,62 | | Tmem201 | transmembrane protein 201 |
| -1,86 | | Slco3a1 | solute carrier organic anion transporter family, member 3a1 |
| -1,64 | | Tcf20 | transcription factor 20 |
| -1,64 | | Ppm1h | protein phosphatase 1H |
| -1,56 | | Bpil3 | BPI fold containing family B, member 6 |
| -1,46 | | Ppa2 | pyrophosphatase 2 |
| -1,55 | | Veph1 | ventricular zone expressed PH domain homolog 1 |
| -1,71 | | Bpifb4 | BPI fold containing family B, member 4 |
| -1,52 | | Gpr124 | G protein-coupled receptor 124 |
| -1,65 | | Pde6d | phosphodiesterase 6D, cGMP-specific, rod, delta |

Stribl_Fig. 10

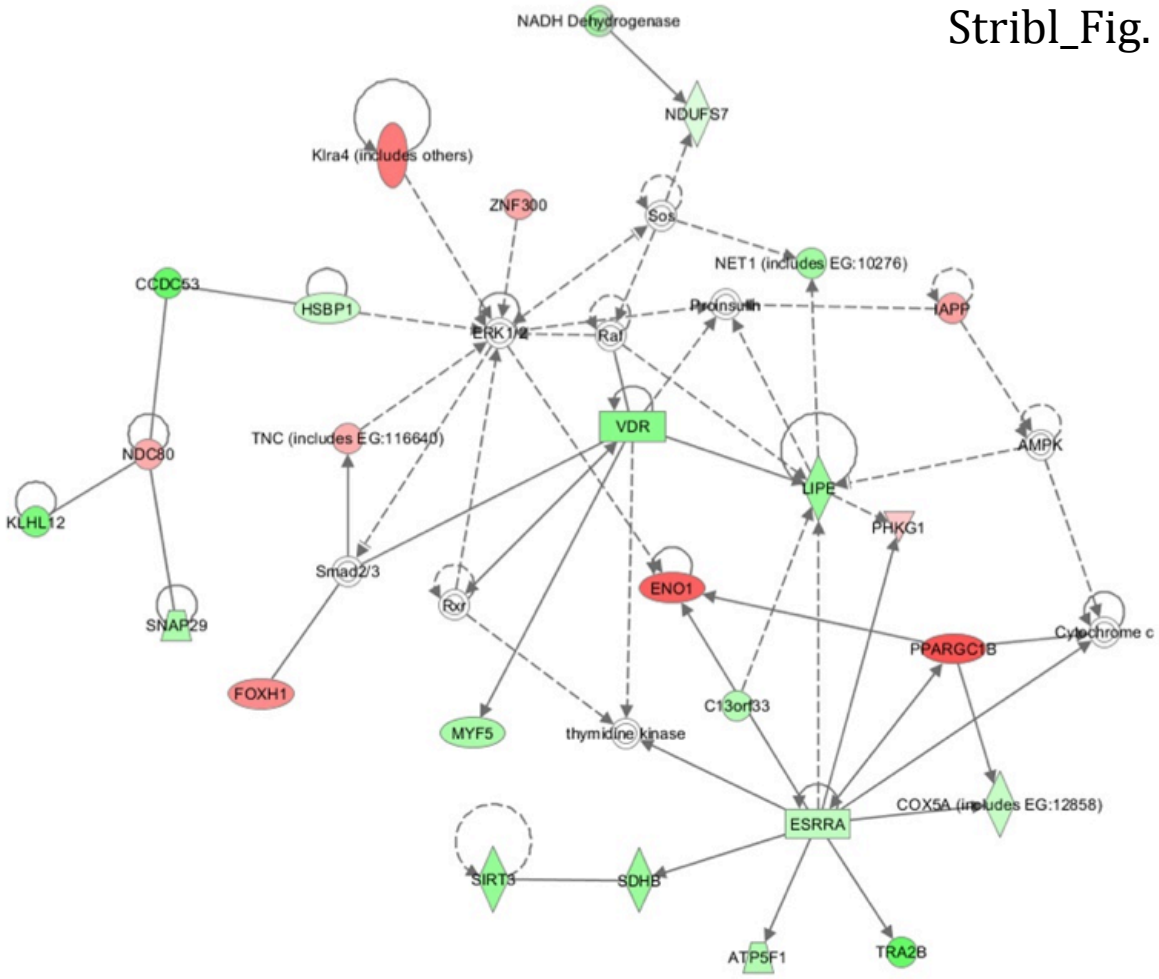

Stribl_Fig. 11